JOURNAL OF MATERIALS SCIENCE 26 (1991) 2608–2614

Effect of additives on some properties of silicon oxynitride ceramics

M. OHASHI, S. KANZAKI, H. TABATA
Government Industrial Research Institute, Nagoya, 1-1 Hirate-cho, Kita-ku, Nagoya 462, Japan

Silicon oxynitride ceramics are formed by reaction sintering of silicon nitride and silica with certain metal oxide additives. The reaction rate during sintering and the subsequent properties of silicon oxynitride are affected by the quantity and kinds of additives. The reaction rate increased for addition of equal molar amounts of ZrO_2, ZrO_2(+ 2.8 mol % Y_2O_3), $AlO_{1.5}$, $LnO_{1.5}$, CeO_2, MgO, in that order (where Ln = Nd, Sm, Gd, Dy, Er, Yb and Y). The lanthanide oxide (1.5 mol %)-doped silicon oxynitride ceramics had a high fracture toughness, because crack deflection occurred due to the precipitation of an intergranular crystalline phase with a high thermal expansion coefficient compared with silicon oxynitride. The oxidation rate was higher with an increasing quantity of additive. In samples containing an intergranular crystalline phase, stability of the crystalline phase is an important factor and could impair the oxidation resistance of silicon oxynitride ceramics.

1. Introduction

Silicon oxynitride ceramics are formed by reaction-sintering of silicon nitride and silica with certain metal oxide additions to promote densification. As with other engineering ceramics such as silicon nitride [1], β-sialon [2] and silica-rich mullite [3], silicon oxynitride ceramics are formed by a process of liquid-phase sintering [4]. The liquid phase remains as a secondary intergranular phase, and limits the potential properties of these ceramics. We have investigated the thermal and mechanical properties [4–7] and oxidation behaviour [7, 8] of ceria-doped silicon oxynitride ceramics containing intergranular phases with different properties. In this study, an attempt was made to prepare the silicon oxynitride ceramics by hot-pressing Si_3N_4–SiO_2 mixed powders with various additives (MgO, Al_2O_3, ZrO_2, ZrO_2 (2.8 mol % Y_2O_3) and Ln_2O_3, where Ln = Nd, Sm, Gd, Dy, Er, Yb, Y and Ce, added as CeO_2), and to investigate (i) the effect of the additives on the rate of the reaction to form silicon oxynitride and (ii) some properties of the ceramic materials.

2. Experimental procedure

The starting Si_3N_4 powder (Denki Kagaku Kogyo K. K., Japan) had oxygen and total metallic impurity contents of 1.2 wt % and 153 p.p.m., respectively, and a specific surface area of 22 $m^2 g^{-1}$. This powder was composed of 95.6% α-Si_3N_4 and 4.4% β-Si_3N_4. The starting SiO_2 powder and metal oxide powders (except MgO), derived from alkoxides and calcined at 600 to 700 °C for 1 h, had a purity of 99.99% (Hokko Chemical Industry Co. Ltd, Japan). MgO powder was obtained by calcining $Mg(OH)_2$ (MH-30; Iwatani Chemical Industry Co. Ltd, Japan) at 900 °C for 1 h.

For the formation of Si_2N_2O, an equimolar ratio of Si_3N_4/SiO_2 is required. Therefore, the amount of oxygen in the Si_3N_4 powder has to be counted as another SiO_2 source. Each metal oxide powder sintering aid was added to the equimolar Si_3N_4/SiO_2 mixture at 1 to 50 mol %. The mixture was vibrationally milled for 6 h in methanol using a silicon nitride container and balls. After drying, the mixed powder was passed through a 60 mesh sieve, and then hot-pressed under 29 MPa at 1700 °C for 2 h in a 0.1 MPa nitrogen atmosphere. The heating rate was 10 °C min^{-1}.

Three-point flexural strength was measured at room temperature to 1400 °C on bars 3 × 3 × 26 mm, ground with a No. 400 diamond wheel and chamfered with a No. 600 diamond disc. A span of 20 mm was used with a crosshead speed of 0.5 mm min^{-1}. Fracture toughness (K_{IC}) was measured by the indentation microfracture (IM) method. It was calculated using the equation of Marshall and Evans [9]. Young's modulus was measured by an ultrasonic pulse echo method. Bulk density was measured by Archimedes' method using distilled water. Crystalline phases present were identified by X-ray diffraction (XRD) (Cu$K\alpha$, 40 kV, 100 mA) and the fraction of Si_2N_2O formed, $Si_2N_2O/(Si_3N_4 + Si_2N_2O)$, was quantified by XRD.

3. Results and discussion

Table I shows bulk density, Young's modulus, K_{IC}, flexural strength (MOR) from room temperature to 1400 °C, weight gain by oxidation at 1400 °C for 100 h and the fraction of silicon oxynitride formed, $Si_2N_2O/(Si_3N_4 + Si_2N_2O)$, for the silicon oxynitride ceramics with various metal oxide additives.

0022-2461/91 $03.00 + .12

TABLE I Properties of silicon oxynitride ceramics with various metal oxide additives

Additive (mol %)		Bulk density ($g\,cm^{-3}$)	Young's modulus (GPa)	K_{IC} ($MN\,m^{-3/2}$)	MOR (MPa)			Weight gain 1400 °C/100 h ($10^{-4}\,g\,cm^{-2}$)	Fraction reacted (%)
					RT	1200 °C	1400 °C		
CeO_2	2.0	2.87	236	2.4	672	773	768	0.30	84
	3.0	2.90	239	5.2	740	199	–	10.40	99
Nd_2O_3	1.0	–	–	–	–	–	–	0.30	–
	1.5	2.90	238	4.2	709	205	–	3.23	99
Sm_2O_3	1.0	2.87	239	2.3	576	664	578	0.31	–
	1.5	2.90	241	3.2	638	247	–	6.72	99
Gd_2O_3	1.0	–	–	–	–	–	–	0.28	–
	1.5	2.92	243	4.1	706	301	–	3.29	96
Dy_2O_3	1.0	2.88	237	2.4	600	686	626	0.29	–
	1.5	2.93	239	4.4	705	203	–	3.75	96
Er_2O_3	1.0	–	–	–	–	–	–	0.27	–
	1.5	2.93	242	4.3	688	222	–	4.95	97
Yb_2O_3	1.0	2.88	239	2.3	580	735	637	0.31	–
	1.5	2.93	243	5.4	681	157	–	7.09	–
Y_2O_3	1.0	–	–	–	–	–	–	0.30	–
	1.5	2.87	240	5.1	655	230	–	3.07	91
MgO	0.5	2.84	221	2.7	481	739	586	2.43	53
	1.0	2.82	236	1.9	524	672	509	2.82	84
	2.0	2.82	243	2.5	493	356	86	6.97	98
	3.0	2.83	243	2.5	613	445	82	7.83	98
	5.0	2.85	241	2.4	645	386	105	12.70	98
Al_2O_3	2.5	2.80	231	2.2	581	745	565	0.90	84
	5.0	2.80	234	2.3	694	473	314	1.50	95
	7.5	2.82	233	–	684	–	–	2.42	96
	10.0	2.81	231	2.1	653	384	245	2.90	97
	20.0	2.86	229	2.4	480	461	312	3.44	98
	30.0	2.90	230	2.2	542	592	424	3.92	98
	50.0	2.96	227	2.5	492	662	544	3.96	98
ZrO_2	2.0	2.87	209	2.9	542	713	–	–	26
	3.0	2.89	206	2.9	487	619	–	1.36	31
	5.0	2.93	207	3.1	528	704	–	1.29	39
	10.0	3.00	212	3.1	434	688	–	1.35	54
	30.0	3.25	227	3.1	740	545	359	4.32	86
	50.0	3.44	223	3.3	597	598	482	28.20	94
$ZrO_2 + Y_2O_3$	3.0	2.89	219	2.6	425	564	578	1.23	58
	10.0	2.99	235	3.1	474	678	632	1.21	83
	50.0	3.54	229	2.9	624	554	489	29.70	–

3.1. Ln_2O_3 additions

The mechanical properties [4–7] and oxidation behaviour [7, 8] of CeO_2-doped silicon oxynitride ceramics have already been reported. With other lanthanide oxide additions (Nd_2O_3, Sm_2O_3, Gd_2O_3, Dy_2O_3, Er_2O_3, Yb_2O_3, Y_2O_3), the properties of the silicon oxynitride ceramics were almost the same as those of the ceria-doped material. The eutectic points in the various Ln_2O_3–SiO_2 systems are at 1625 to 1680 °C [10], and nitrogen ions as an additional component lower the eutectic temperature by 100 to 150 °C [1, 11, 12]. Therefore, a liquid forms above $\simeq 1500\,°C$ in the various Ln–Si–O–N systems, and promotes densification and formation of Si_2N_2O. The fraction of Si_2N_2O formed in the 1.5 mol % Ln_2O_3-doped specimens decreased slightly with decreasing rare-earth ionic radii ($Ce^{3+} > Nd^{3+} > Sm^{3+} > Gd^{3+} > Dy^{3+} > Er^{3+} > Yb^{3+}$) as shown in Table I. The fraction formed with 1.5 mol % Y_2O_3 is much less. These results are affected by the different eutectic temperatures in the various Ln–Si–O–N systems which increase as the rare-earth ionic radius decreases [11].

In the case of 3.0 mol % CeO_2 addition, which on reaction releases oxygen to give 1.5 mol % Ce_2O_3, the Ce_2O_3/SiO_2 ratio of the intergranular phase increased as the formation of Si_2N_2O proceeded. On cooling, the intergranular liquid phase remained as a glass until the Ce_2O_3/SiO_2 ratio exceeded a certain level ($\simeq 0.6$) at which point the liquid phase crystallized as $Ce_{4.67}(SiO_4)_3O$–$Ce_5(SiO_4)_3N$ solid solution during cooling [3, 4]. However, crystallization of the intergranular phase did not occur in the specimen with 2.0 mol % CeO_2, hot-pressed under the same conditions, because the Ce_2O_3/SiO_2 ratio did not reach the previous level for formation of the apatite [4].

With other lanthanide oxide additions, the intergranular phases in the 1.5 mol % Ln_2O_3-doped specimens crystallized as $Ln_{4.67}(SiO_4)_3O$–$Ln_5(SiO_4)_3N$ solid solution, but those in the 1.0 mol % Ln_2O_3-doped specimens remained as amorphous phases on cooling. There were great differences in mechanical properties (flexural strength, K_{IC}) and oxidation behaviour (weight gain by oxidation at 1400 °C for 100 h) between the specimens with 1.0 mol % Ln_2O_3 and those with 1.5 mol % Ln_2O_3, as shown in Table 1. These results seemed to depend on the difference in thermal and mechanical properties between the intergranular glassy phase and the crystalline apatite. The thermal expansion coefficient of the intergranular glassy phase with ceria addition (4 to $5 \times 10^{-6}\,°C^{-1}$) was estimated [7] to be slightly larger than that of Si_2N_2O ($a = 1.26 \times 10^{-6}$, $b = 3.89 \times 10^{-6}$, $c = 3.99 \times 10^{-6}\,°C^{-1}$ [13]). On the other hand, the thermal expansion coefficient of the intergranular crystalline phase $Ln_5(SiO_4)_3N$ was assumed to be similar to that of $La_5(SiO_4)_3N$ ($10.1 \times 10^{-6}\,°C^{-1}$ [14]). The crack propagated along the intergranular crystalline phase–silicon oxynitride interface in the specimens with 1.5 mol % Ln_2O_3, whereas it propagated transgranularly in the specimens with 1.0 mol % Ln_2O_3 containing only amorphous intergranular phases. It must be concluded that interfacial bonding between Si_2N_2O and the intergranular crystalline phase was weakened due to the large thermal expansion mismatch and, therefore, crack deflection occurred in the 1.5 mol % Ln_2O_3-doped specimens causing an increase in fracture toughness.

Fig. 1 shows the temperature dependence of flexural strength of two Ln_2O_3-doped Si_2N_2O ceramics (Ln = Sm, Dy). The dependence was also influenced by the difference in properties of the intergranular phases. The strength of the 1.0 mol % Ln_2O_3-doped specimens remained almost steady up to 1400 °C (600 MPa). It may be noted that the softening temperature of the intergranular glassy phases was very high. However, the strength of the 1.5 mol % Ln_2O_3-doped specimens fell sharply above 1200 °C. The intergranular phases were crystallized as $Ln_5(SiO_4)_3N$ to a considerable extent during cooling; the $Ln_2Si_2O_7$ phase was also identified in the case of Er_2O_3, Yb_2O_3 and Y_2O_3 additions. The intergranular crystalline phases at the surface tended to be unstable during testing in air. In the case of CeO_2, $Ce_5(SiO_4)_3N$ within the bulk was decomposed to an amorphous phase and a small amount of $Ce_2Si_2O_7$ after annealing in dry air as low as 700 °C for 20 h. This same crystalline phase at the surface was decomposed after annealing at 500 °C for 20 h. The other $Ln_5(SiO_4)_3N$ phases were stable in air up to higher temperatures, compared with $Ce_5(SiO_4)_3N$. However, the phases at the surface were slightly decomposed by oxidation during the bending test at 1200 °C, and a small amount of $Ln_2Si_2O_7$ was formed. In the case of Sm_2O_3 and Gd_2O_3 additions, no $Ln_2Si_2O_7$ was observed by XRD, but the peaks for the apatite phase shifted slightly following the oxidation. It is concluded that a compositional shift occurred to $Ln_{4.67}(SiO_4)_3O$ within the $Ln_5(SiO_4)_3N$–$Ln_{4.67}(SiO_4)_3O$ solid-solution range with loss of nitrogen. It is suggested that the degradation of strength at 1200 °C is due to the instability of the intergranular crystalline phase. It is also possible that residual intergranular glassy films containing large concentrations of impurity elements, which remained at the grain boundaries following crystallization, are responsible for the degradation of strengths at high temperatures.

Fig. 2 shows the weight gains of the 1.0 and 1.5 mol % Ln_2O_3-doped Si_2N_2O ceramics after oxidation at 1400 °C for 100 h in dry air. The weight gains of the 1.0 mol % Ln_2O_3-doped samples were very small compared with the 1.5 mol %-doped samples and also compared with other non-oxide ceramics [7]. Only cristobalite was formed on the surface of the 1.0 mol %-doped silicon oxynitride containing only intergranular glassy phases above 1000 to 1100 °C. Outward diffusion of Ln^{3+} ions was not observed in the specimens. This reveals that the diffusion rate of the Ln^{3+} ion is very low in these intergranular glassy phases in the specimens. On the other hand, during oxidation of the 1.5 mol %-doped samples containing intergranular crystalline phases, $Ln_2Si_2O_7$ precipitated in addition to cristobalite. With ceria addition, $Ce_2Si_2O_7$ was produced within the bulk by the decomposition of $Ce_5(SiO_4)_3N$, and CeO_2 was formed at the surface. Furthermore, the 3.0 mol % ceria-doped specimen showed the lowest oxidation resistance of all the lanthanide oxide-doped specimens containing the $Ln_5(SiO_4)_3N$ phases. This resulted from the ability of the Ce^{3+} ion to be oxidized to $Ce4^+$. The lower oxidation resistance of the 1.5 mol %-doped specimens was ascribed to the release of Ln^{3+} by decomposition of $Ln_5(SiO_4)_3N$, which also involves loss of nitrogen, and the faster diffusion path for Ln^{3+} along grain-boundary glassy films left after crystallization.

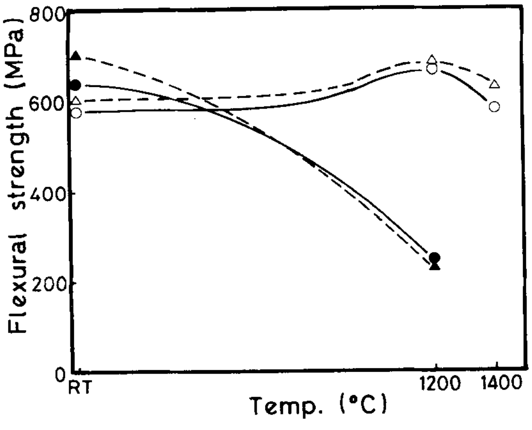

Figure 1 Flexural strength as a function of temperature for silicon oxinitride ceramics with lanthanide oxides: (○) 1.0 and (●) 1.5 mol % Sm_2O_3, (△) 1.0 and (▲) 1.5 mol % Dy_2O_3.

3.2. MgO addition

The eutectic temperature at 1390 °C [1] in the MgO–SiO_2–Si_3N_4 system is the lowest temperature for liquid formation compared with the other metal oxide additions. The reaction rate for silicon oxynitride formation using equimolar amounts of all the additives was the highest for MgO (Fig. 3).

The intergranular phase remained as a glass on cooling even when 10 mol % MgO was added. Therefore, toughening by the precipitation of a crystalline phase with a large thermal expansion coefficient in the intergranular region was not observed in the specimens with MgO additive (Table I). Fig. 4 shows the flexural strength of the Si_2N_2O ceramics with 1, 3 and 5 mol % MgO as a function of temperature. Degradation of strength in the high-temperature range was

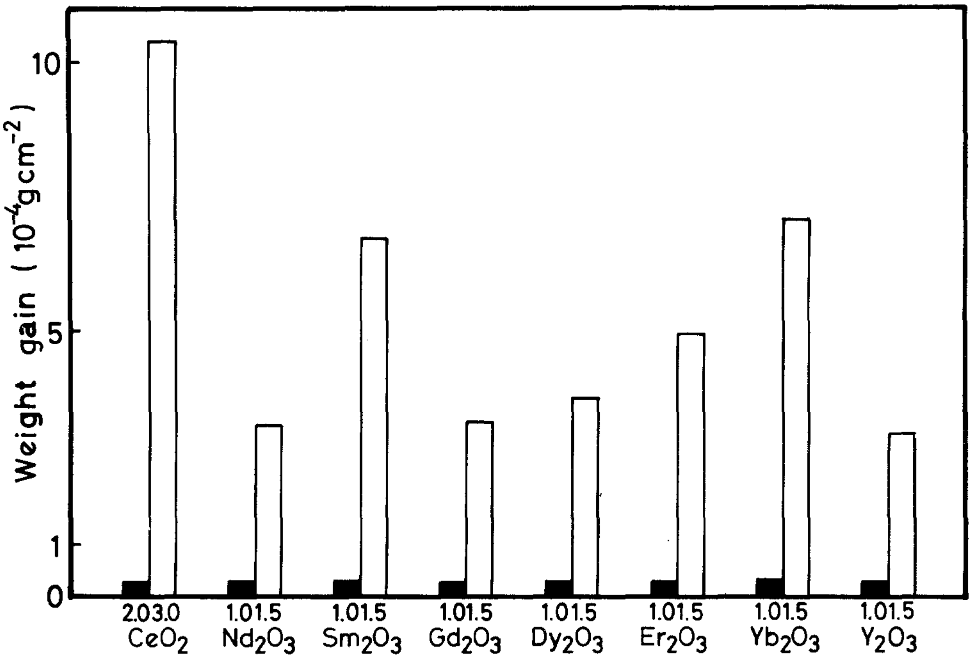

Figure 2 Weight gain of silicon oxynitride ceramics with (■) 1.0 and (□) 1.5 mol % lanthanide oxide by oxidation in dry air at 1400 °C for 100 h.

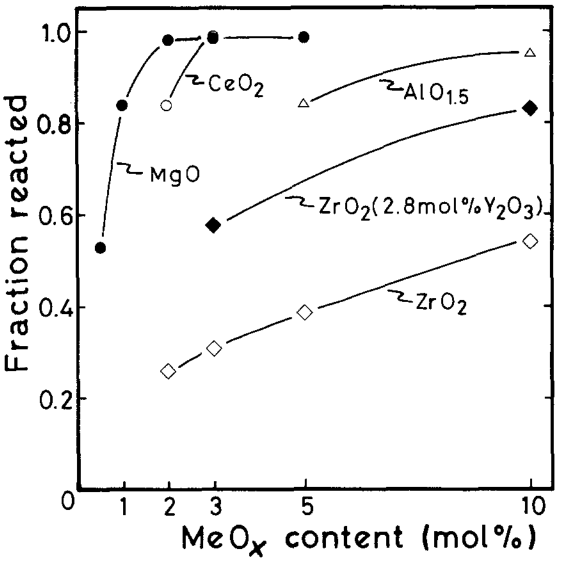

Figure 3 Fraction of silicon oxynitride formed, $Si_2N_2O/(Si_3N_4 + Si_2N_2O)$, in specimens hot-pressed at 1700 °C for 2 h as a function of additive content: (●) MgO, (○) CeO_2, (△) $AlO_{1.5}$, (◇) ZrO_2, (◆) ZrO_2 (2.8 mol % Y_2O_3).

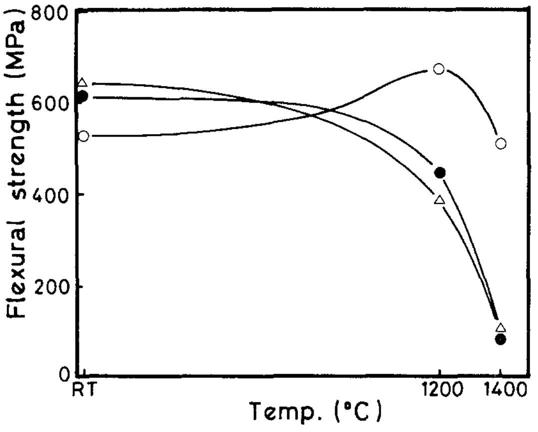

Figure 4 Flexural strength as a function of temperature for silicon oxynitride ceramics with magnesium oxide: (○) 1, (●) 3 and (△) 5 mol %.

accelerated with increasing amounts of MgO additive. This is because the softening temperature of the intergranular glassy phases decreased with increasing MgO/SiO_2 ratio, which is higher with larger amounts of MgO addition. The high-temperature strength of the 2.0 mol % MgO-doped sample was sharply reduced compared with that of the 1.0 mol % MgO-doped silicon oxynitride.

The weight gain of the MgO-doped silicon oxynitride samples after oxidation at 1400 °C for 100 h increased as the amount of MgO additive increased (Fig. 5). This is because the outward diffusion of the Mg^{2+} ion became faster with an increasing concentration of the ion in the intergranular glassy phase, corresponding to an increase in the amount of MgO which reduces the glass viscosity. α-cristobalite and Mg_2SiO_4 were detected in the oxidized scales of all the specimens. The formation of Mg_2SiO_4 was particularly enhanced in the specimens containing more than 2.0 mol % MgO. The weight gain of the samples with MgO was larger than for the silicon oxynitride samples containing an equimolar amount of the other additives (Table I). It is suggested that the diffusion rate of Mg^{2+} in the magnesium silicon oxynitride glass is higher than for the Ln^{3+}, Al^{3+} and Zr^{4+} ions in the corresponding oxynitride glasses.

3.3. Al_2O_3 addition

The Al_2O_3–SiO_2–Si_3N_4 system has a eutectic point at 1470 °C [1] to 1480 °C [15]. The temperature is approximately the same as the eutectic temperatures with lanthanide oxide additions. However, the reaction to form Si_2N_2O with Al_2O_3 addition was sluggish, compared with that with the CeO_2 addition as shown in Fig. 3. It is considered that this resulted

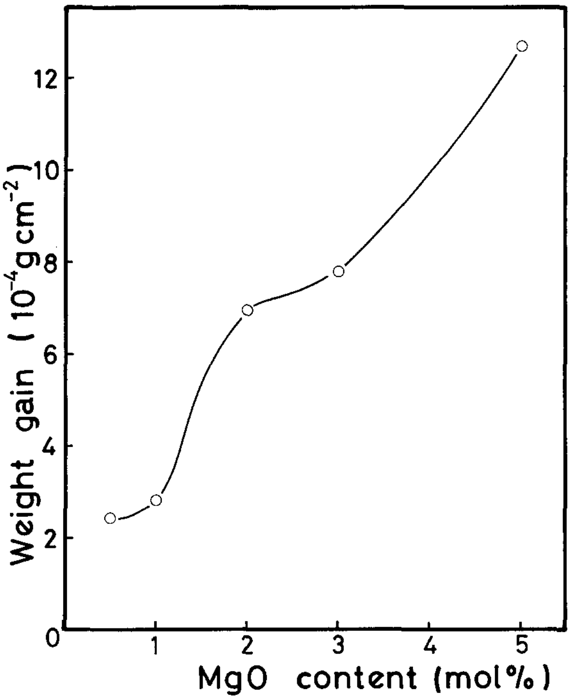

Figure 5 Weight gain of silicon oxynitride ceramics with magnesium oxide by oxidation in dry air at 1400 °C for 100 h.

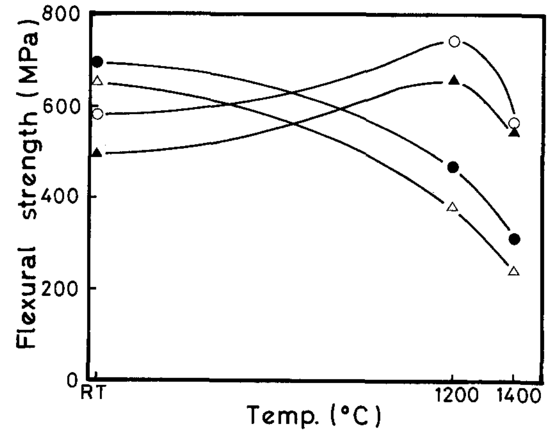

Figure 6 Flexural strength as a function of temperature for silicon oxynitride ceramics with aluminium oxide: (○) 2.5, (●) 5.0, (△) 10.0 and (▲) 50.0 mol %).

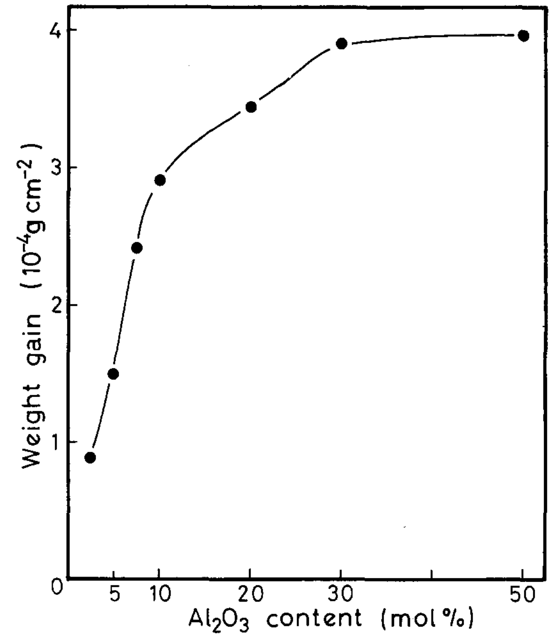

Figure 7 Weight gain of silicon oxynitride ceramics with aluminium oxide by oxidation in dry air at 1400 °C for 100 h.

from the difference in nitrogen solubility and/or diffusion rate of nitrogen in the different oxynitride melts.

No secondary crystalline phase was observed in 2.5 to 7.5 mol % Al_2O_3-doped samples, but the X-phase [2, 15] appeared in silicon oxynitride containing more than 10 mol % Al_2O_3. However, the K_{IC} value was not improved by the formation of the crystalline phase as was the case for the lanthanide oxide additions where N-apatite was formed (Table I). The temperature dependence of flexural strength of the Al_2O_3-doped samples was also influenced by the amount of additive (Fig. 6). At 1200 and 1400 °C, a strength minimum was observed for the 10.0 mol % Al_2O_3-doped sample. Strength degradation at elevated temperatures could be avoided with both smaller and larger amounts of Al_2O_3 addition. These data suggest that the composition of the intergranular glassy phase of the 10.0 mol % Al_2O_3-doped sample was closer to the eutectic composition.

The weight gains after oxidation for 100 h in dry air at 1400 °C for the silicon oxynitride samples containing Al_2O_3 are shown in Fig. 7. The resistance to oxidation is lowered by increasing the quantity of the additive, as observed in the case of MgO addition. The existence of α-cristobalite was confirmed in the oxidized surface of 2.5 to 20.0 mol % Al_2O_3-doped specimens. For 30.0 and 50.0 mol % Al_2O_3-doped samples, mullite was identified instead of α-cristobalite. Fig. 8 shows the backscattered electron image and the elemental distribution of sodium for a cross-section of the 20.0 mol % Al_2O_3-doped silicon oxynitride after oxidation. In the case of the oxidation of the Al_2O_3-doped samples, a liquid with a low melting point and a low viscosity was formed on the sample surface. Fig. 8 clearly shows that the formation of this liquid was dependent on outward diffusion of alkaline ions such as Na^+ or K^+. It is improbable that the starting Al_2O_3 powder contained a large amount of sodium. Further, K_2O and Na_2O are unstable in melts containing Si_3N_4 and SiO_2 [16]. This result suggests that alkaline ions tended to dissolve more easily into the oxynitride glass containing aluminium ions, or the diffusion rate of alkaline ion was higher in this glass. The weight gains for the silicon oxynitride series containing Al_2O_3 were smaller than those for the other oxide additions, because the liquid played a role as an excellent protective layer against oxidation.

3.4. ZrO_2 and ZrO_2 (2.8 mol % Y_2O_3) additions

The ZrO_2–SiO_2–Si_3N_4 system has a eutectic temperature at 1590 °C [1]. This temperature is the highest of those in all the systems examined in this study. The reaction rate for Si_2N_2O formation in this system was very low as compared with those for the other oxide additions (Fig. 3). The rate increased by addition of a small amount of Y_2O_3 to the system, as shown in the

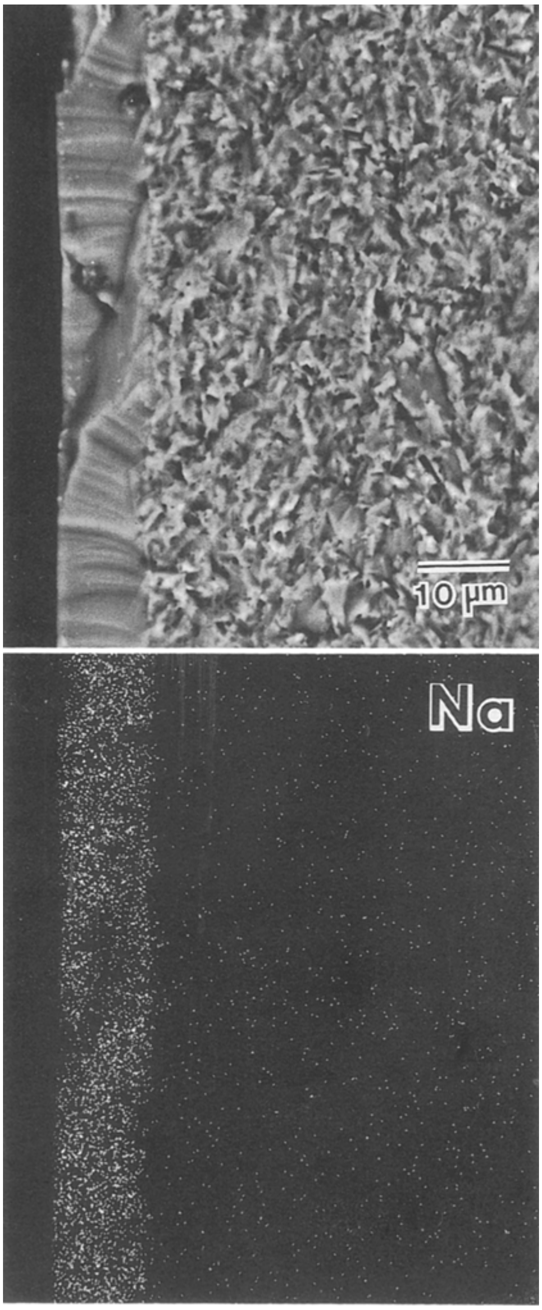

Figure 8 Backscattered electron image and elemental distribution of sodium for a cross-section of 20 mol % Al_2O_3-doped Si_2N_2O ceramic oxidized at 1400 °C for 100 h.

case of ZrO_2 (+ 2.8 mol % Y_2O_3) (partially stabilized zirconia, PSZ).

By analogy with the SiO_2–ZrO_2 phase diagram [17], the eutectic composition of the system containing nitrogen is also located close to silica-rich compositions. Therefore, some ZrO_2 or PSZ particles did not dissolve in the liquid but remained as dispersed particles in the Si_2N_2O matrix, even when a small amount of the oxide was added. However, these dispersed particles did not contribute to toughening of the matrix as indicated in Table I. The strength of the ZrO_2- or PSZ-doped specimens remained almost steady or fluctuated to a slight extent up to 1200 or 1400 °C, because the softening temperature of intergranular glassy phases in the specimens was very high. At 1400 °C, plastic deformation occurred for the specimens with 2.0 to 10.0 mol % ZrO_2 which contained less than 50% of Si_2N_2O and a large volume of the glassy phase. After oxidation at 1400 °C for 100 h, α-cristobalite and $ZrSiO_4$ were identified on the sample surfaces. $ZrSiO_4$ was the major product formed on the surface of the silicon oxynitride samples with additions of 50 mol % ZrO_2 and 50 mol % PSZ, and consequently these samples exhibited large weight gains.

4. Conclusions

The rate of reaction to form silicon oxynitride during reaction sintering of silicon nitride and silica in the presence of various metal oxide additives is affected by the chemical composition of the liquid phase formed. The liquid remained as an intergranular phase, and dominated the mechanical properties and the oxidation behaviour of the bulk body.

The reaction rate to form Si_2N_2O was low for addition of ZrO_2 and increased for equimolar additions of PSZ, $1/2Al_2O_3$, $1/2Ln_2O_3$ and MgO, in that order.

The silicon oxynitride ceramics containing an intergranular glassy phase had K_{IC} values of about 2 to 3 $MN\,m^{-3/2}$, regardless of the amount and the kind of additive. The 1.5 mol % Ln_2O_3-doped specimens (where Ln = Ce, Nd, Sm, Dy, Er, Yb, Y) which contained the intergranular crystalline apatite solid solution $Ln_5(SiO_4)_3N$–$Ln_{4.67}(SiO_4)_3O$, with a high thermal expansion coefficient compared with the silicon oxynitride matrix, had high fracture toughness due to crack deflection.

The strength of the specimens with a small amount of additive remained almost steady up to 1400 °C. It is suggested that the softening temperature of the intergranular SiO_2-rich glassy phase was very high. The high-temperature strength decreased with increasing amounts of additive, except in the case of Al_2O_3 addition, where the high-temperature strength increased with larger amounts of additive. The strength of the 1.5 mol % Ln_2O_3-doped samples fell sharply at 1200 °C. This was related to the crystallization of the intergranular apatite phase on cooling and the stability of this crystalline phase in air under the testing conditions.

The oxidation resistance of silicon oxynitride decreased with an increasing amount of additive. Specimens with an intergranular glassy phase containing mobile cations such as Mg^{2+}, which have a high diffusion coefficient in the glassy phase, were susceptible to rapid oxidation. In the case of the specimens with the intergranular crystalline phase, the stability of this crystalline phase was one of the most important factors affecting the oxidation behaviour.

Acknowledgements

We sincerely thank Professor Stuart Hampshire (University of Limerick, Ireland) for extremely helpful advice and discussions, and we are grateful to Mr Senshu Mitachi (Hokko Chemical Industry Co. Ltd, Japan) for providing the starting oxide powders.

References

1. S. HAMPSHIRE and K. H. JACK, *Proc. Br. Ceram. Soc.* **31** (1981) 37.
2. K. H. JACK, in "Non-Oxide Technical and Engineering Ceramics", edited by S. Hampshire (Elsevier Applied Science, London, 1986) p. 1–30.
3. S. KANZAKI, O. ABE, M. OHASHI and H. TABATA, in Proceedings of 2nd International Symposium, "Ceramic Materials and Component for Engines", Lübeck-Travemünde, FRG. Edited by W. Bunk and H. Hausner (Verlag Deutsche Keramische, Gesellschaft, 1986) p. 625–631
4. M. OHASHI, S. KANZAKI and H. TABATA, *Seramikkusu Ronbunshi* **96** (1988) 1073.
5. M. OHASHI, H. TABATA and S. KANZAKI, *J. Mater. Sci. Lett.* **7** (1988) 339.
6. *Idem*, in Proceedings of International Symposium for the Science of Sintering, Tokyo, Japan, 1987, edited by S. Somiya, M. Shimada, M. Yoshimura and R. Watanabe (Elsevier Applied Science, 1988) p. 1094–1099.
7. M. OHASHI, S. KANZAKI and H. TABATA, *J. Amer. Ceram. Soc.* in press.
8. *Idem*, in Proceedings of 1989 Annual Meeting of the Ceramic Society of Japan (2G15) p. 376.
9. D. B. MARSHALL and A. G. EVANS, *J. Amer. Ceram. Soc.* **64** (1981) C182.
10. "Phase Diagrams for Ceramists", 1969 Supplement (The American Ceramic Society, Inc., OH, USA).
11. G. E. GAZZA, in "Progress in Nitrogen Ceramics", edited by F. L. Riley (Nijhoff, 1983) p. 273.
12. L. J. GAUCKLER, H. HOHNKE and T. Y. TIEN, *J. Amer. Ceram. Soc.* **63** (1980) 35.
13. M. B. HENDERSON and D. TAYLOR, *Trans. Br. Ceram. Soc.* **74** (1975) 49.
14. M. MITOMO, F. IZUMI, S. HORIUCHI and Y. MATSUI, *J. Mater. Sci.* **17** (1982) 2359.
15. I. K. NAIK, L. J. GAUCKLER and T. Y. TIEN, *J. Amer. Ceram. Soc.* **61** (1978) 332.
16. R. E. LOEHMAN, *J. Non-Cryst. Solids* **56** (1983) 123.
17. W. C. BUTTERMAN and W. R. FOSTER, *Amer. Mineralogist* **52** (1967) 880.

*Received 23 January
and accepted 6 June 1990*